Hydrogen-Bond Breaking and Proton Exchange in Collisions of Gaseous Formic Acid with Liquid Sulfuric Acid

Jane K. Klassen* and Gilbert M. Nathanson†

Gas-liquid scattering experiments provide direct observations of the fate of hydrogen-bonding molecules striking the surfaces of acidic liquids. Collisions of gaseous formic acid with concentrated sulfuric acid show that impinging monomers (HCOOH and DCOOD) scatter inelastically from the interface or become trapped by surface H_2SO_4. Most trapped DCOOD molecules undergo proton exchange before desorbing from the acid, indicating that gas-surface accommodation almost always leads to reaction with H_2SO_4 molecules. This proton transfer is not inhibited by dimerization of the formic acid: The dimers readily undergo intramolecular hydrogen bond cleavage and D-H exchange before desorbing from the acid.

The first step in the dissolution of a gas molecule occurs at the surface of a liquid. During the initial encounter, the impinging gas molecule can scatter away from the surface or dissipate its incident energy before momentarily coming to rest at the interface. Our goal is to learn what happens after a molecule is trapped by the surface of a reactive liquid like sulfuric acid. We address the trapping, reaction, and desorption steps that occur in many gas-liquid processes, ranging from the industrial absorption of olefins in sulfuric acid to the hydrolysis of nitrogen and chlorine species in atmospheric aerosols (*1*). An incoming molecule DX (Fig. 1) may scatter off the surface of concentrated sulfuric acid in one or a few bounces (direct inelastic scattering), react on a single collision, or be deflected enough times along a rough surface to dissipate its energy and be trapped at the interface (*2*). The accommodated molecule may either desorb immediately from the acid without reaction (trapping-desorption) or remain long enough to undergo protonation and perhaps further reaction (*3, 4*). In the case of protonation (5), the solvated species DXH^+ may remain within solution (long-time solvation) or decompose into HX, which can then desorb into the vacuum (trapping-reaction-desorption).

The pathways can be investigated by choosing DX to be formic acid monomer or dimer because these species can undergo proton exchange and are weak enough bases for protonation to be reversible on a 0.05-s measurement time scale (*6, 7*). The scattering experiments reveal two distinct signatures of reactivity between gas and liquid: (i) proton exchange between DCOOD and H_2SO_4 to generate desorbing DCOOH and (ii) acid-induced dissociation of the hydrogen bonds in $(HCOOH)_2$ and $(DCOOD)_2$. The data demonstrate that formic acid monomers and dimers trapped by interfacial H_2SO_4 almost always undergo sufficient solvation for protonation and hydrogen-bond breaking to occur.

The experiments were carried out by directing nearly monoenergetic beams of the monomer (HCOOH or DCOOD) or dimer $[(HCOOH)_2$ or $(DCOOD)_2]$ at 98.8 weight % (18.5 M) sulfuric acid. At this azeotrope composition, sulfuric acid is composed of neutral and ionic species dominated by hydrogen-bonded H_2SO_4 molecules (*8*). We created films of clean sulfuric acid (vapor pressure $< 10^{-4}$ torr) inside a vacuum chamber by partially immersing a glass wheel in a Teflon reservoir filled with the acid (*9*). The wheel rotated at 0.5 Hz, picking up a 0.3-mm film. A glass blade then scraped away the outermost 0.1 mm of the acid, leaving behind a fresh 0.2-mm-thick layer of liquid. This continuously renewed film passed by a hole in the reservoir (12 mm in diameter), where it intercepted the gas beam for 0.05 s. Time-of-flight (TOF) velocity analysis was used to record the time for the recoiling and desorbing species to travel from a chopper wheel, positioned just after the surface, to a mass spectrometer 19.2 cm from the wheel. The incident beam was directed at the acid surface at an angle of 45°, and the exiting molecules were detected at an exit angle of 45°. We varied the incident translational energies E_{inc} of the molecular beams between 14 and 170 kJ/mol by bubbling N_2, He, and H_2 through formic acid and expanding the gas mixture through a pinhole nozzle. We varied the dimer fraction from nearly one to nearly zero by heating the nozzle from 30° to 200°C. In the mass spectrometer, the dimers preferentially ionized into $(HCOOH)H^+$ or $(DCOOD)D^+$, and the monomers were monitored as $HCOOH^+$, $DCOOD^+$, or $DCOOH^+$.

The TOF spectrum of formic acid scattering from sulfuric acid (Fig. 2) is bimodal at E_{inc} = 84 kJ/mol (17 times the average room-temperature collision energy of 5 kJ/mol). The fast peak (time of arrival ~200 μs) corresponds to formic acid molecules scattering inelastically from the surface; these molecules on average transfer 70% of their incident energy to the liquid during the collision. The slow shoulder (peak time of arrival ~415 μs) matches a thermal distribution at the sulfuric acid temperature of 295 K, indicating that some HCOOH molecules are trapped by the acid and that a fraction of these accommodated molecules desorb back into the vacuum (*7, 10*). In contrast, a more basic molecule like D_2O shows no evidence of thermal desorption. As previously shown (*3*), nearly all trapped D_2O molecules dissolve for long times in the acid, prohibiting observation of the HOD or H_2O reaction products.

We can distinguish between the physical process of trapping-desorption and the chemical process of trapping-reaction-desorption by substituting DCOOD for

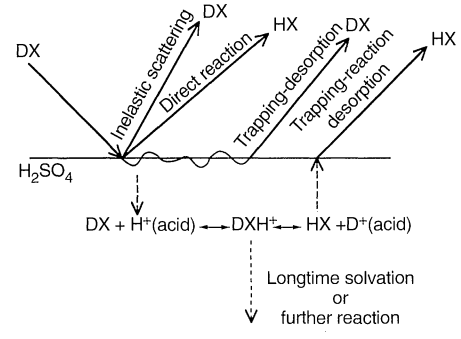

Fig. 1. Five pathways for a deuterated molecule, DX, striking sulfuric acid, H_2SO_4.

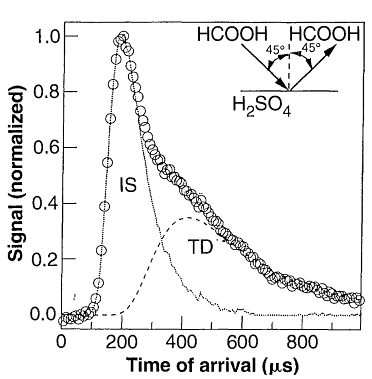

Fig. 2. Time-of-flight spectra of formic acid at E_{inc} = 84 kJ/mol scattering from sulfuric acid. IS and TD refer to direct inelastic scattering and thermal desorption of the exiting formic acid molecules. (**Inset**) Scattering geometry.

Department of Chemistry, University of Wisconsin, 1101 University Avenue, Madison, WI 53706, USA.

---

*Present address: Molecular Physics Laboratory, SRI International, Menlo Park, CA 94025, USA.

†To whom correspondence should be addressed.

HCOOH and searching for evidence of proton exchange in the desorbing products. We recorded TOF spectra at $DCOOD^+$ and $DCOOH^+$ after collisions of incident DCOOD with H_2SO_4 at E_{inc} = 97 kJ/mol (Fig. 3) (*11*). The reagent DCOOD molecules scatter in a narrow distribution of velocities typical of inelastic scattering, with only a small shoulder attributable to thermal desorption. The thermal peak reappears when product DCOOH is monitored by the mass spectrometer. The ratio of the intensities of the thermal desorption components, $I_{thermal}(DCOOH^+)/I_{thermal}(DCOOD^+)$, is at least 3:1, indicating that proton exchange typically takes place before the formic acid molecules can desorb into the vacuum (*12*). The trapping of formic acid molecules by concentrated sulfuric acid is thus more often a chemical process involving solvation and reaction as opposed to a solely physical process involving only energy accommodation.

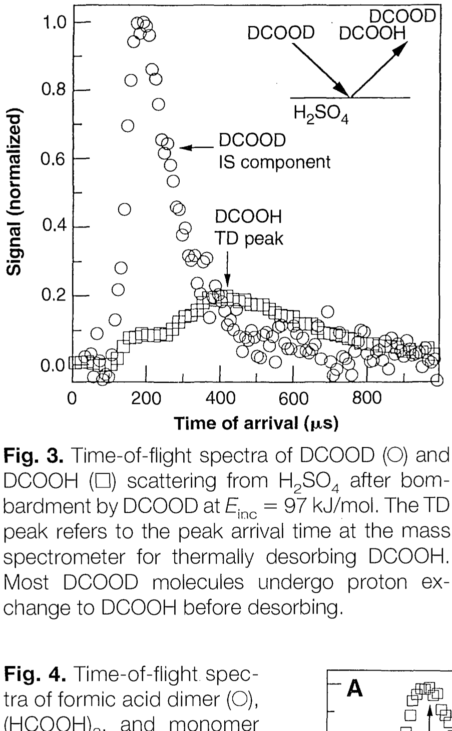

Fig. 3. Time-of-flight spectra of DCOOD (○) and DCOOH (□) scattering from H_2SO_4 after bombardment by DCOOD at E_{inc} = 97 kJ/mol. The TD peak refers to the peak arrival time at the mass spectrometer for thermally desorbing DCOOH. Most DCOOD molecules undergo proton exchange to DCOOH before desorbing.

The DCOOH TOF spectrum also displays a fast bump under the inelastic peak of DCOOD (time of arrival ~200 μs). This bump has the same peak arrival time as the inelastic component of the DCOOD spectrum, suggesting that it arises from contaminant DCOOH in the incident beam and not from proton transfer through a direct collision. This explanation is supported by the intensity ratio $I_{inelastic}(DCOOD^+)/I_{inelastic}(DCOOH^+)$ of ≈0.06, which is close to the ion ratio measured for the incident beams of ≈0.08. Thus, we have no distinct evidence for proton exchange mediated by direct collisions that bypass the trapping process.

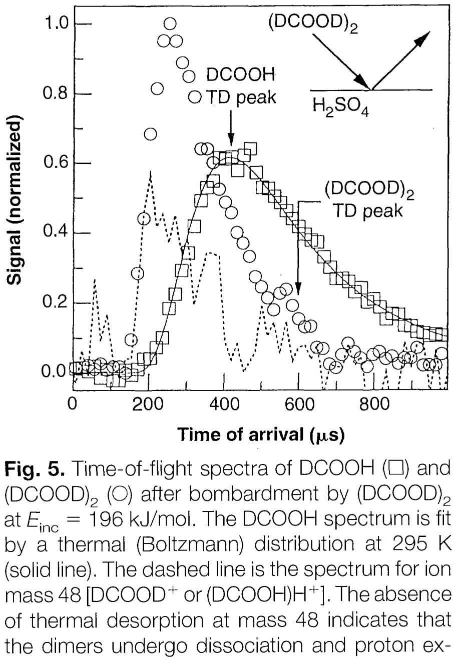

Fig. 5. Time-of-flight spectra of DCOOH (□) and $(DCOOD)_2$ (○) after bombardment by $(DCOOD)_2$ at E_{inc} = 196 kJ/mol. The DCOOH spectrum is fit by a thermal (Boltzmann) distribution at 295 K (solid line). The dashed line is the spectrum for ion mass 48 [$DCOOD^+$ or $(DCOOH)H^+$]. The absence of thermal desorption at mass 48 indicates that the dimers undergo dissociation and proton exchange to DCOOH before desorbing.

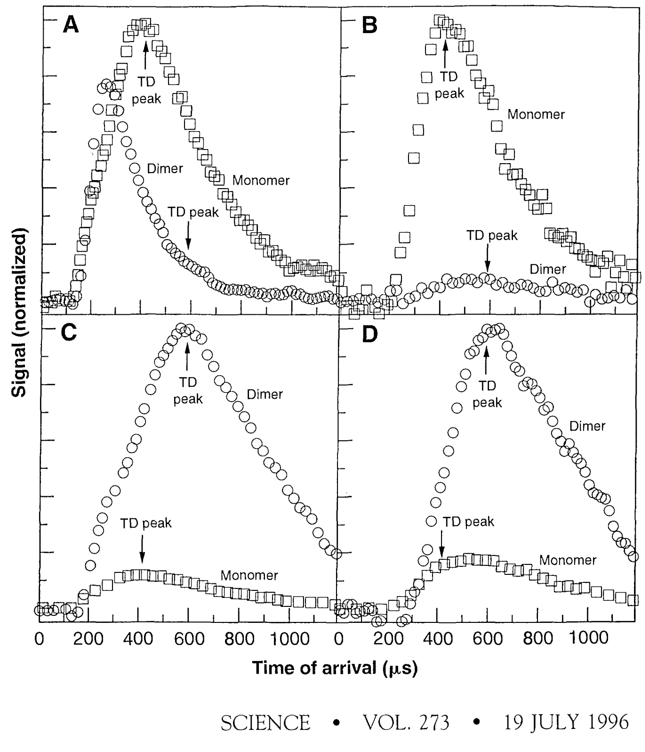

Fig. 4. Time-of-flight spectra of formic acid dimer (○), $(HCOOH)_2$, and monomer (□), HCOOH, after bombardment by $(HCOOH)_2$ dimer at (**A**) E_{inc} = 155 kJ/mol from H_2SO_4, (**B**) E_{inc} = 14 kJ/mol from H_2SO_4, (**C**) E_{inc} = 155 kJ/mol from squalane, and (**D**) E_{inc} = 14 kJ/mol from squalane. Thermally accommodated dimers survive intact when desorbing from squalane but are cleaved into monomers by sulfuric acid.

The trapping and reaction of formic acid molecules with sulfuric acid are likely to be initiated by hydrogen bonding between HCOOH and surface H_2SO_4 after the gas molecule dissipates most of its energy. We attempted to impede trapping and reaction by prebonding the C=O and O–H groups in formic acid through dimerization of the monomers. These cyclic dimers are bound by two hydrogen bonds with a dissociation enthalpy of 64 kJ/mol (*13*). The dimer still possesses reactive sites on each O atom, but monomer desorption must now proceed through dimer bond cleavage (*14*). In TOF spectra recorded for $(HCOOH)_2$ striking sulfuric acid at E_{inc} = 155 and 14 kJ/mol (Fig. 4, A and B, respectively), thermal desorption is dominated by monomers and not by dimers. The monomer ion/dimer ion ratios of the thermal desorption signals, $I_{thermal}(HCOOH^+)/I_{thermal}(HCOOH{\cdot}H^+)$, are ≈10 and ≈25 at E_{inc} = 155 and 14 kJ/mol, respectively (*15*). In contrast, the ion ratios for the incoming beams, $I_{incident}(HCOOH^+)/I_{incident}(HCOOH{\cdot}H^+)$, are 0.08 at E_{inc} = 155 kJ/mol and 0.02 at E_{inc} = 14 kJ/mol. The dominance of monomers in thermal desorption indicates that dimer trapping is accompanied by dissociation of the dimers into monomers. This breakup does not appear to be specifically induced by high-energy collisions because dimer dissociation occurs at incident kinetic energies well below the bond strength of the dimer (Fig. 4B).

To determine if dimer breakup occurs in collisions with nonreactive liquids as well, we scattered $(HCOOH)_2$ off squalane ($C_{30}H_{62}$), a long-chain hydrocarbon liquid (Fig. 4, C and D). The trends are opposite to those of sulfuric acid: For squalane, thermal desorption is dominated by dimers, and there is little dimer breakup even at high collision energies. Most formic acid dimers survive the accommodation process intact in collisions with a nonreactive liquid. In contrast, sulfuric acid cleaves the dimers into monomers before desorption can take place.

The ultimate fate of the dimers is revealed by $(DCOOD)_2$ scattering at E_{inc} = 170 kJ/mol (Fig. 5). The dimers can scatter inelastically but do not undergo desorption if they are trapped by sulfuric acid. Thermal desorption is instead dominated by proton-exchanged DCOOH monomers. To determine if the dimer can fall apart without proton exchange or if it can undergo proton exchange without dissociation, we monitored the signal at mass 48 (dashed line). This mass corresponds to DCOOD$^+$ from DCOOD monomer and to (DCOOH)H$^+$ from doubly proton-exchanged dimer. The fast arrival times in the mass-48 spectrum indicate that the signal arises mostly from contaminant DCOOD monomer in the incident beam scattering inelastically from the acid, and not from (DCOOD)$_2$ reactions with the acid leading to thermally desorbing DCOOD or (DCOOH)$_2$. The three spectra demonstrate that only directly scattered dimers survive intact, whereas trapped dimers undergo both dissociation and proton exchange before the monomers desorb from the acid.

These experiments reveal that reactions with H_2SO_4 nearly always accompany the thermal accommodation of formic acid monomers and dimers on the surface of sulfuric acid. We expect chemical reactions to follow trapping if H_2SO_4 molecules within the collision zone can reorient rapidly enough to hydrogen bond to the formic acid monomer or dimer before thermal motions propel the molecules back into the gas phase (*16*). Subsequent proton transfer would then occur either within an interface that is a few molecules thick or be delayed until the formic acid molecules diffuse deeper into the acid. The observation of proton exchange in collisions between formic acid molecules and sulfuric acid implies that solvation and protonation may often be intermediate steps in the trapping and desorption of protic gas species.

REFERENCES AND NOTES

1. S. K. Chaudhuri and M. M. Sharma, *Ind. Eng. Chem. Res.* **30**, 339 (1991); D. R. Hanson and E. R. Lovejoy, *Science* **267**, 1326 (1995).
2. J. E. Hurst *et al.*, *Phys. Rev. Lett.* **43**, 1175 (1979); C. T. Rettner, E. K. Schweizer, C. B. Mullins, *J. Chem. Phys.* **90**, 3800 (1989); M. E. Saecker and G. M. Nathanson, *ibid.* **99**, 7056 (1993).
3. S. T. Govoni and G. M. Nathanson, *J. Am. Chem. Soc.* **116**, 779 (1994).
4. See also J. H. Hu *et al*, *J. Phys. Chem.* **99**, 8768 (1995); E. D. Guldan, L. R. Schindler, J. T. Roberts, *ibid.*, p. 16059; K. B. Eisenthal, *Acc. Chem. Res.* **26**, 636 (1993).
5. M. Eigen, *Angew. Chem. Int. Ed. Engl.* **3**, 1 (1964); K. Ando and J. T. Hynes, *J. Mol. Liq.* **64**, 25 (1995); and references therein.
6. The basicity of formic acid, as gauged by the acid dissociation constant *K* of the protonated base, is *K*(formic acid·H$^+$) ≈ $10^{8.7}$. Formic acid is much less basic than water because *K*(H_2O·H$^+$) = 10^0. See M. Liler, *Reaction Mechanisms in Sulfuric Acid* (Academic Press, New York, 1971), p. 256.
7. Uptake measurements indicate that roughly 60% of the impinging formic acid molecules dissolve in and remain within the acid during the 0.05-s observation time of the surface (K. M. Fiehrer and G. M. Nathanson, in preparation).
8. R. A. Cox, *J. Am. Chem. Soc.* **96**, 1059 (1974).
9. S. A. Lednovich and J. B. Fenn, *AIChE J.* **23**, 454 (1977).
10. Some formic acid molecules in solution may decompose into CO + H_2O. We could detect only a very noisy signal for CO desorption, in part because of a large background at the CO$^+$ mass due to residual N_2. See K. W. Smith, R. M. Noyes, P. G. Bowers, *J. Phys. Chem.* **87**, 1514 (1983).
11. We expect that proton exchange of DCOOD leads to DCOOH and not HCOOD. A search for double proton exchange revealed no evidence of desorbing HCOOH at mass 46 after correction for signal from desorbing DCOOH and DCOOD dissociatively ionizing into DCOO$^+$.
12. The lower limit of 3 : 1 is imposed by the noise in the DCOOD spectrum. The ratio of the TD intensities at a 45° exit angle should reflect the angle-integrated TD ratio because the TD channels typically follow nearly identical, cosine-like angular distributions.
13. J. Chao and B. J. Zwolinski, *J. Phys. Chem. Ref. Data* **7**, 363 (1978).
14. Enhanced nonpairwise, cooperative effects are expected to increase the basicity of the dimer over the monomer. R. Zhang and C. Lifshitz, *J. Phys. Chem.* **100**, 960 (1996); A. E. Reed, L. A. Curtiss, F. Weinhold, *Chem. Rev.* **88**, 899 (1988).
15. At lower impact energies, the monomer ion/dimer ion ratio increases as more dimers become trapped and dissociate into monomers.
16. I. Benjamin, M. A. Wilson, A. Pohorille, G. M. Nathanson, *Chem. Phys. Lett.* **243**, 222 (1995).
17. We thank F. Weinhold for discussions concerning hydrogen bonding and K. Fiehrer for the formic acid uptake measurement. This work was supported by NSF (CHE-9417909) and Presidential Young Investigator and Dreyfus Teacher-Scholar Awards to G.M.N.

18 March 1996; accepted 20 May 1996

The Morphogenesis of Bands and Zonal Winds in the Atmospheres on the Giant Outer Planets

James Y-K. Cho and Lorenzo M. Polvani

The atmospheres of Jupiter, Saturn, Uranus, and Neptune were modeled as shallow layers of turbulent fluid overlying a smooth, spherical interior. With only the observed values of radius, rotation rate, average wind velocity, and mean layer thickness as model parameters, bands and jets spontaneously emerged from random initial conditions. The number, width, and amplitude of the jets, as well as the dominance of anticyclonic vortices, are in good agreement with observations for all four planets.

Despite vast differences in chemical composition, thermodynamic properties, physical size, rotation rate, and orientation, the atmospheres of the four Jovian planets exhibit a remarkable similarity in their banded appearance and the associated strong zonal (east-west) winds. This unexpected similarity is at present a major unanswered question (*1*, *2*). Here we address this question with a single unifying dynamical framework to determine how many of the observed large-scale features of the Jovian atmospheres can be captured by a very simple physical model.

We assumed that the Jovian atmospheres can be modeled with a nearly inviscid, hydrostatically balanced, thin layer of turbulent fluid under the influence of gravitational and Coriolis forces. The motion of such a fluid (*3*) is governed by the shallow-water equations

$$\frac{\partial \mathbf{v}}{\partial t} + \mathbf{v}\cdot\nabla\mathbf{v} + f\mathbf{k}\times\mathbf{v} = -g\nabla h \qquad (1)$$

$$\frac{\partial h}{\partial t} + \nabla\cdot(h\mathbf{v}) = 0 \qquad (2)$$

where $\mathbf{v}$ is the horizontal velocity, t is time, h is the height of the fluid, $f = 2\Omega\sin\varphi$ is the Coriolis parameter, g is the gravitational acceleration, Ω is the rotation rate of the planet, φ is the latitude, and $\mathbf{k}$ is the unit vector normal to the surface of the sphere. For all four planets, h is taken starting from just below the visible cloud decks at an approximately 1000-mbar level; this is the level at which the planetary radius is commonly measured. Equations 1 and 2 were solved in spherical geometry with the use of a high-resolution, pseudospectral, parallel code (*4*). Similar equations have been used to model latitudinally confined features, principally Jupiter's Great Red Spot, in annular and channel geometries (*5*). In contrast, we extend the shallow-water model to comprise the entire planetary surface and apply it to all four planets.

The computations presented here are initialized with a random turbulent flow. The initial vorticity of this flow (Fig. 1A) is the same for all four planets, and the results are insensitive to the scale of the initial vorticity structures, provided it is chosen to be small. These computations, performed at a grid resolution of 0.7°, are essentially inviscid since more than 97% of the initial energy is conserved throughout the evolution.

The advantage of using this simple model is that only five parameters need to be specified (Table 1): Ω, g, the planetary radius a, the characteristic velocity scale U, and the mean height of the fluid layer H. The overall amplitude of the initial energy spectrum is controlled by U; the Rhines scale (*6*) L_β is

---

Program in Applied Mathematics and Department of Applied Physics, Columbia University, New York, NY 10027, USA.